

Unoccupied electronic states in graphite

V. Dose, G. Reusing, and H. Scheidt,

Physikalisches Institut der Universität, D-8700 Würzburg, Germany

(Received 25 January 1982)

Soft x-ray appearance potential (SXAP) and ultraviolet bremsstrahlung measurements have been employed to explore the density of unoccupied electronic states of graphite. Deconvolutions of SXAP spectra are in quite good agreement with theoretical predictions. Considerable differences between earlier isochromat results obtained at $\hbar\omega_0=1$ keV and the present measurements at $\hbar\omega_0=9.7$ eV are explained in terms of a symmetry-dependent energetic variation of the radiative transition-matrix element. As a consequence, neither x-ray nor uv isochromat reflect the density of empty states over the full 20-eV region considered here satisfactorily. A properly weighted average of the respective data, however, agrees quite well with theory and SXAP deconvolution.

I. INTRODUCTION

Segregation of carbon to Pt surfaces at elevated temperatures is known to be an annoying obstacle in preparation of clean Pt surfaces. The carbon Auger signal from segregated carbon layers on Pt is quite similar to that observed from pure graphite.¹ Low-energy electron diffraction (LEED) observations of carbon-covered Pt(100) surfaces have revealed hexagonal patterns and ring structures^{2,3} indicating a high degree of order of the carbon overlayers. Lattice constants deduced from these measurements are in accord with those of bulk graphite.² This indicates that the graphite grows in layers parallel to the Pt(100) surface, and we therefore consider the growth of graphite on Pt(100) to be a particularly easy method of obtaining highly oriented graphite samples suitable for band-structure spectroscopy.

Considerable work has been carried out on the valence-band structure of graphite. Beyreuther and Wiech⁴ and Kieser⁵ performed x-ray emission experiments. Analysis of the direction of polarization of the emitted x rays shows σ and π components of states originating from atomic p states. Feuerbacher *et al.*^{6,7} found a π -band splitting of 0.8 eV at Q and P points of the Brillouin zone with the use of photoemission. Photoemission measurements by Bianconi *et al.*⁸ at quantum energies in the range of 33–200 eV show pronounced differences of the energy dependence of the transition matrix elements for states with atomic s -like or p -like symmetry, respectively. Angle-resolved photoemission was employed by Williams *et al.*⁹ They determine the dispersion of the highest occu-

ried π band along the Γ - Q direction (near the Q point) of the Brillouin zone. Available x-ray photoemission spectra (XPS) results^{5,10,11} do not reflect as in the case of metals the valence-band density of states but rather the s -like character density. This results from the above-mentioned different energy dependence of the transition matrix elements for states with different symmetry. It follows from this collection of results that there is no single unique approach to determine the valence-band density of states of graphite. The situation will be shown to be similarly complicated for the conduction band.

Much less information is thus far available on the conduction-band density of states. Highly excited states have been investigated by Willis *et al.*^{7,12} employing secondary electron emission. Fine structure in the spectra was assigned to valence-electron excitations into unoccupied bands and interpreted on the basis of a two-dimensional band-structure calculation by Painter and Ellis.¹³ Willis *et al.*¹² have shown that the extension of these theoretical calculations to the three-dimensional case leads to band splittings of the order of 1 eV.

Soft x-ray appearance potential spectroscopy (SXAPS) and bremsstrahlung isochromat spectroscopy (BIS) are more suitable tools to approach the conduction-band structure especially since they also cover the otherwise inaccessible energy region between Fermi and vacuum level. Moreover, the interpretation of results obtained with these methods does not presume a knowledge of the valence-band structure. SXAPS results on graphite have been obtained by several groups in the past.^{14–18} How-

ever, their interpretation has until recently remained a matter of controversy. The original interpretation of the multiplex structure as plasmon losses must be abandoned after the work of Houston¹⁹ and Webb.¹⁸ Their interpretation of the spectrum in terms of density of states only is strongly supported by the results of this work.

Isochromat measurements in the x-ray region have been reported by Kieser²⁰ and Baer.¹¹ Neither experiment reproduces the density of unoccupied states which lead Kieser to invoke a complicated energy-loss model. As will be shown in the subsequent section, BIS measurements in the ultraviolet quantum-energy region add valuable information to those in the x-ray region and bring about an interpretation consistent with the calculated theoretical density of empty states.

II. APPEARANCE POTENTIAL AND uv-BREMSSTRAHLUNG ISOCHROMAT SPECTROSCOPY (SXAPS, BIS)

Park and Houston^{21,22} revived in the late sixties this very old technique and by application of modulation and phase-sensitive detection techniques devised a modern surface scientific spectroscopy. In SXAPS the total soft x-ray intensity emitted by a sample under electron bombardment is measured as a function of electron energy. With increasing electron energy, there occur small increases of the x-ray yield at energies corresponding to the binding energy of core electrons. At threshold for core-level excitation, both the incident and the excited core electron are scattered to empty states immediately above the Fermi level of the sample. Assuming constant transition matrix elements and sharp initial states, the rate of core-hole production $P(E)$ is proportional to the autoconvolution of the conduction-band density of empty states $N(E)$. Experimentally, x radiation is recorded to monitor the rate of core-hole production and the slowly varying background of noncharacteristic bremsstrahlung is conveniently removed employing the potential modulation differentiation technique. The resulting line shape is given by

$$\frac{dP(E)}{dE} \sim \frac{d}{dE} \int_0^E N(\epsilon)N(E-\epsilon)d\epsilon, \quad (1)$$

E being the excess energy over threshold. This spectroscopic technique has been widely used to determine core-level binding energies. Further, because of the extremely simple and unique spectra

as compared to Auger electron spectra (AES), it still has its merits as a tool for chemical analysis especially when applied to multiple component alloys.^{23,24} SXAPS has also been shown to respond to adsorption phenomena.²⁵⁻²⁷ Chemisorption and oxidation phases could be distinguished. The most interesting application however, the derivation of the density of states from the signal shape, has only recently been made accessible. Efficient and numerically stable inversion procedures for the integral equation (1) have become available.^{28,29} Results for some $3d$ and $5d$ metals showing excellent agreement with theoretical calculations have been published elsewhere.³⁰⁻³²

The experimental setup used in this work deviates from the conventional type in two respects. We use a high gain CsI x-ray photocathode instead of gold or stainless steel. Extremely high long-term stability of the spectrometer is obtained by automatic modulation frequency control via a phase-locked loop.³⁰

In isochromat spectroscopy the bremsstrahlung yield of a sample under electron bombardment is measured at a fixed quantum energy $\hbar\omega_0$ as a function of incident electron energy. Radiative transitions of the electron may be regarded as inverse photoemission.^{33,34} Electrons with initial energy E with respect to the Fermi level of the anode which undergo a radiative transition with emission of a quantum $\hbar\omega_0$ occupy final states in the conduction band of the sample at an energy $E - \hbar\omega_0$. Assuming again constant transition matrix elements, the intensity of radiation with energy $\hbar\omega_0$ will be proportional to the density of final states. This simple model has been shown to be valid for isochromat results in the x-ray energy range, where the method can be regarded as inverse to XPS.³⁵⁻³⁷

The electron energy E is given by

$$E = \phi + eV + E_{th}, \quad (2)$$

where ϕ is the cathode work function, V the externally applied voltage, and E_{th} the mean thermal energy of electrons emitted by the cathode. The threshold for detection of radiation $\hbar\omega_0$ is given by

$$eV = \hbar\omega_0 - \phi - E_{th} \quad (3)$$

and fixes the position of the Fermi level on the energy scale independent from the work function of the sample.

The spectrometer employed in this work operates at a quantum energy of $\hbar\omega_0 = 9.7 \pm 0.3$ eV, an energy in the ultraviolet region at which BIS must be regarded as inverse to ultraviolet photo-

emission spectra (UPS). It uses an energy selective Geiger Müller counter instead of the "classical" x-ray monochromator.³⁸ As a consequence, we obtain sensitivities higher by a factor of 10^4 as compared to conventional setups.

Results on clean polycrystalline metallic samples of the $3d$ and $5d$ elements have been published previously^{31–33,39} and have confirmed the above-outlined simple model for the elementary process in these cases even at such a low quantum energy if additional electron-hole pair production is properly accounted for.³⁹

III. SAMPLE PREPARATION

Experiments were carried out in a UHV system with a base pressure of 10^{-8} Pa. The system included an isochromat spectrometer, an SXAP spectrometer, an argon-ion gun, and a quadrupole residual gas analyzer. SXAP and isochromat spec-

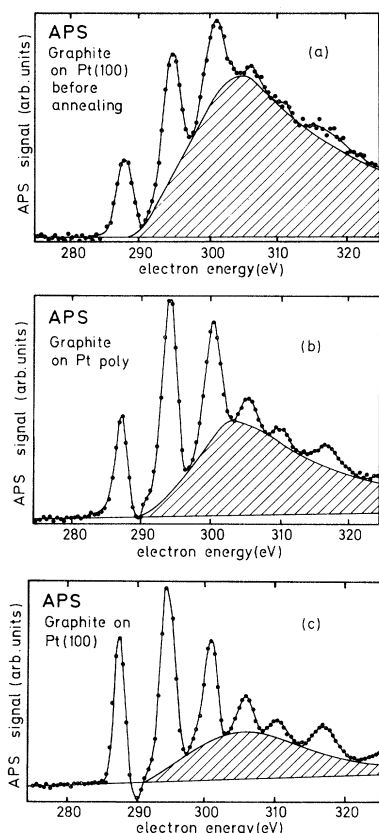


FIG. 1. Appearance potential spectra of graphite on platinum substrates. Parts (a), (b), and (c) represent states of increasing crystallographic perfection of the graphite overlayer. Note in particular the increasing intensity in the first peak of the multiplex spectrum and the simultaneously decreasing, slowly varying (dashed) contribution to the overall signal.

trometers have been described in detail earlier.^{30,38} A Pt(100) single crystal as well as a polycrystalline Pt sample were mounted on the manipulator. Carbon, the prominent contamination on both samples, was removed by prolonged oxidation at 10^{-4} Pa and 1500 K. Subsequent argon sputtering produced, by the SXAPS standards, the clean final state of the sample. Controlled growth of carbon was achieved by adsorption of benzene under electron bombardment at 1 keV energy and 2 mA/cm^2 current density. The sample temperature was 1150 K under these conditions. Transformation of the adsorbed carbon to graphite required annealing at 1400 K for about an hour. Isochromat and SXAP spectra were always taken before and after the annealing cycle.

IV. GROWTH OF GRAPHITE ON PLATINUM

Carbon (1s) SXAP spectra referring to different sample states are displayed in Figs. 1(a)–1(c). The typical graphite multiplex spectrum^{14,15} is clearly visible in all cases, however, with a different degree of perfection. The spectrum in Fig. 1(a) corresponds to graphite on Pt(100) before annealing. Figs. 1(b) and 1(c) refer to polycrystalline platinum and Pt(100) after annealing. They are characteristic for a steady state since neither further annealing nor increased annealing temperature resulted in a further change. From the BIS measurement

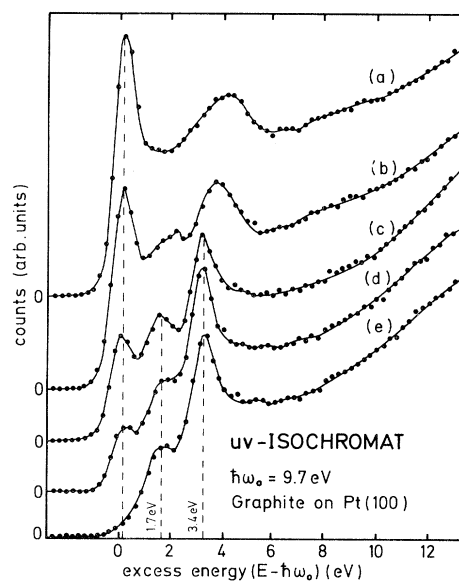


FIG. 2. Ultraviolet isochromates from a platinum (100) single crystal with graphite overlayers. Curve (a) represents the signal from clean platinum while (e) corresponds to a graphite layer-thickness such that platinum emission is no longer detectable.

below, we estimate a graphite layer thicker than 30 monolayers. We observe a significant increase in intensity of the first peak in the spectrum when going from Fig. 1(a) to Fig. 1(c) while simultaneously the slowly varying contribution to the signal under the multiplex structure [dashed area in Figs. 1(a)–1(c)] decreases. From earlier work by Bradshaw and Menzel,¹⁵ we conclude that the spectra of Figs. 1(a)–1(c) correspond to graphite with increasing degree of perfection, and that Pt(100) constitutes a favorable substrate for growth of well-ordered graphite.

A series of uv isochromats corresponding to graphite layers of increasing thickness on Pt(100) is shown in Fig. 2. The curve in 2(a) refers to the clean platinum sample. Strong *d*-band emission is observed immediately above the Fermi level. Another broad feature at 4 eV has been shown to result from direct optical interband transitions.⁴⁰ The curves in 2(b)–2(e) represent increasing graphite coverage. We observe structures at 1.7 and 3.4 eV while the Pt *d*-band emission fades out simultaneously and is no longer visible in curve *e*. Figure 2(e) should therefore correspond to the uv-isochromat characteristic for pure graphite. A lower limit to the thickness of the graphite layer may be obtained using an electron mean free path of $\lambda \approx 20 \text{ \AA}$ at an energy of 10 eV. If the spectrum of Fig. 2(e) contained a still detectable 1% Pt contribution, the graphite overlayers would be at least 100- \AA thick.

Isochromat spectra are, similar to SXAP spectra, quite sensitive to the degree of order of the carbon

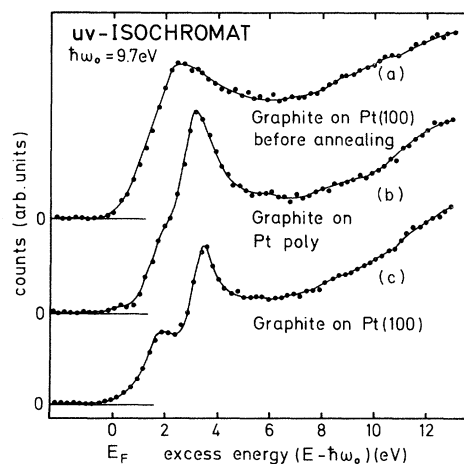


FIG. 3. Ultraviolet isochromats are quite sensitive to the degree of crystallographic perfection of the graphite overlayer. The double peak structure in curve (c) is due to a π -band splitting resulting from interlayer interaction in a well-ordered sufficiently thick overlayer.

overlayer. Isochromats corresponding to the SXAP spectra in Fig. 1 are shown in Figs. 3(a)–3(c). While the signal from the unannealed carbon overlayer [Fig. 3(a)] exhibits only a single broad maximum, two well-resolved peaks are observed in the spectrum from graphite on Pt(100) at 1.7 and 3.4 eV [Fig. 3(c)]. Similar structure but much less pronounced is obtained from graphite on polycrystalline platinum [Fig. 3(b)].

V. DISCUSSION OF RESULTS

Webb *et al.*^{17,18} were actually the first to interpret the graphite multiplex appearance potential spectrum in terms of the graphite band structure only. These conclusions were further supported by subsequent work of Houston,¹⁹ who pointed out the similarity of the appearance potential spectrum with an autoconvolution of an ionization-loss spectrum. Straightforward deconvolution of the appearance potential spectra following Eq. (1) obtained in this work are shown in Figs. 4(a) and 4(b). Figure 4(b) displays the deconvolution result for graphite on Pt(100) as full dots in comparison

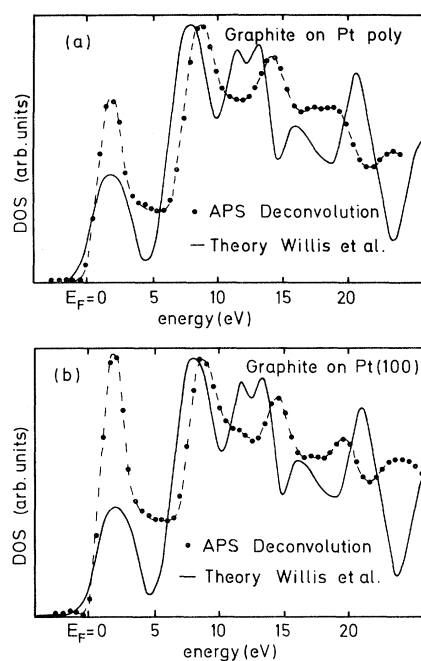


FIG. 4. Deconvolution of appearance potential spectra shown as solid dots is compared to a theoretical density of states calculation smoothed with a 1.8 eV FWHM (full width at half maximum) Gaussian. The general agreement is quite satisfactory. Parts (a) and (b) refer to graphite layers of different degrees of crystallographic perfection. Note the difference in amplitude of the peak at 2 eV above E_F .

to a theoretical calculation by Willis *et al.*¹² Their results, originally presented as a histogram, have been suitably smoothed by convolution with a Gaussian. The agreement between theory and experiment is quite encouraging since every structure in the calculated density of states is reproduced, though minor shifts in the energetic positions are clearly present and show up in the isochromat spectra also (see Fig. 8). These are, however, within the limits of reliability of calculations for highly excited bands. Similar good agreement is obtained for graphite on polycrystalline platinum shown in Fig. 4(a). The main difference as compared to Fig. 4(b) is in the amplitude of the first maximum in the density of states at about 2 eV, where the largest deviation from the theoretical result also shows up in both cases. SXAP spectra obtained by Verhoeven¹⁶ and Webb¹⁸ for various angles of incidence of the primary electrons relative to the graphite *c* axis provide an explanation for the above-mentioned difference. Their spectra exhibit essentially only an attenuation of the first peak in the SXAP spectrum when the angle of incidence of the primary electron is increased from normal. The attenuation is as large as 70% at 45°. The difference in peak heights of the first peak in the appearance potential spectra is therefore attributed to a more uniform *c*-axis orientation of the graphite layer on Pt(100) as compared to the polycrystalline substrate. This is in accord with Webb's suggestion¹⁸ that the matrix element for transitions to these states with (π, p) symmetry in the energy range 0–4 eV above E_F (see Fig. 6) should be strongly angle dependent.

Figure 5 shows a comparison of our uv isochromat with two isochromats obtained at x-ray energies by Kieser²⁰ and Baer,¹¹ respectively. The agreement between the latter two sets of data is

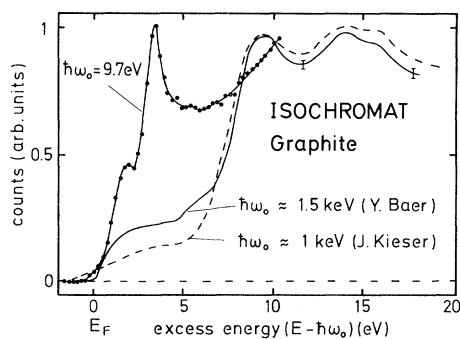


FIG. 5. Graphite isochromat spectra taken at x-ray energies and at 9.7 eV differ considerably. The reason is a symmetry-dependent energetic variation of the radiative transition matrix element.

quite good, apart from the difference in intensity in the range 0–5 eV. The uv isochromat, on the other hand, exhibits considerable structure just in this range. Attempts to explain the structureless region beyond 5 eV by electron-hole pair formation as in the case of 3*d* and 5*d* transition metals³⁹ have failed in the present case. This is tentatively attributed to a breakdown of the random-*K* approximation for graphite. This is not unexpected due to the high anisotropy of this material. The entirely different shape of the uv isochromat compared to those measured in the x-ray region came as a surprise, considering the very good agreement obtained so far for transition metals.^{31,32,39} Again we are led to invoke the anisotropy of graphite. While in-plane bonding proceeds via sp^2 hybridization, the weak interplane bonding is due to p_z orbitals. As a consequence, the band structure in Fig. 6 may be classified in terms of π bands with atomic p character and σ bands from sp^2 hybridized states. The σ bands show a gap of about 12 eV. Within this gap, one finds π bands above and below the Fermi energy which overlap at the *P* point of the Brillouin zone. The weak interlayer interaction leads to a band splitting of the order of 1 eV.

We are now going to refer to XPS and UPS measurements in order to interpret the results of Fig. 5. UPS measurements by Bianconi *et al.*⁸ employing quantum energies between 30 and 200 eV show a strong energy dependence of the transition matrix element. While at low quantum energies the spectra are dominated by transitions from p states, the contribution from s and p states become comparable at 120 eV. At higher energies, s states begin to dominate. This trend is further supported by XPS results. The behavior is in accord with

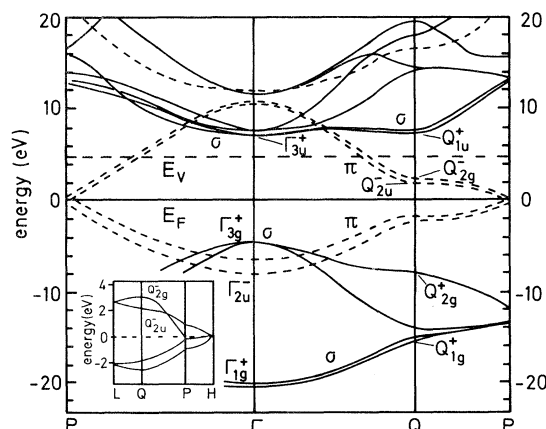


FIG. 6. Calculated band structure of graphite after Refs. 7 and 13.

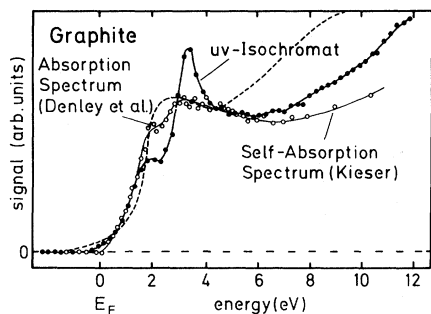


FIG. 7. Ultraviolet isochromat compared to graphite $1s$ absorption spectra as obtained by Kieser (Ref. 5) and Denley *et al.* (Ref. 41).

photoionization cross sections of atomic carbon for initial s and p states, respectively. We now suggest to transfer these symmetry arguments to isochromat or inverse photoemission measurements. This leads us to expect that the ultraviolet isochromat is dominated by transitions into empty p states while x-ray isochromats reflect predominantly transitions into empty s states. This conclusion is further supported by quantum absorption measurements near the carbon K edge which should, due to the dipole selection rules, reflect only the final p state density. A comparison of such measurements by Kieser⁵ and Denley *et al.*⁴¹ with the present uv isochromat is given in Fig. 7. Among Denley's results, only those obtained for microcrystalline graphite with random c -axis orientation lend themselves to a comparison with the present data. Their measurements on poly- and monocrystalline graphite are strongly influenced by additional polarization selection rules leading to strong attenuation of transitions into final π states. Denley's absorption data, however, though in rough overall agreement with the uv isochromat, do not show the π -band splitting presumably due to insufficient crystal size.

Kieser's experiment on x-ray self-absorption in graphite offers more favorable conditions in this respect. X radiation is observed in his setup with polarization vector parallel to the graphite c axis. This arrangement favors transitions in final π

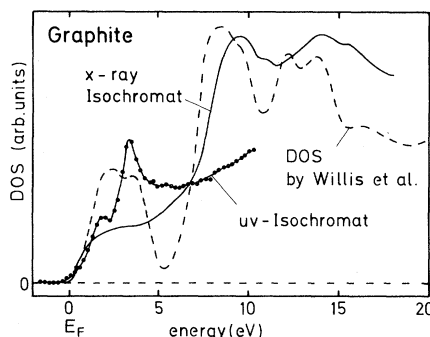


FIG. 8. Properly weighted average of uv and x-ray isochromats exhibits all features predicted by the theoretical density of states calculation. The theoretical data have been smoothed in this case with a 0.4-eV FWHM Gaussian and a Lorentzian of energy-dependent width describing the finite final-state lifetime (Ref. 31). Note that the overall smoothing near E_F is less than in Fig. 4.

states. Since monocrystalline material was used as absorber, an indication of the splitting observed in the uv isochromat is also present in his data.

The foregoing discussion suggests that a properly weighted sum of uv- and x-ray isochromats should provide an experimentally determined density of unoccupied states of graphite. Figure 8 shows that indeed a combination of two such sets of data reproduces all structures predicted by the theoretical calculation in this energy range.¹²

Since there is only one unoccupied band in the energy range $E_F \leq E \leq E_F + 5$ eV (see Fig. 6), the structure in the uv isochromat can be unambiguously attributed to the critical points Q_{2u}^-, Q_{2g}^- with a high density of final states approximately 2–3 eV above E_F . The π -band splitting is reflected by a corresponding double-peak structure in the density of states with a 1.3-eV separation (dashed line, Fig. 8). Experimentally, this splitting turns out to be 1.7 eV. Further support to this interpretation is gained by reinspection of Fig. 3. The double-peak structure of the isochromat is only obtained for graphite on Pt(100) indicating relatively perfect order of adjacent layers.

¹J. T. Grant and T. W. Haas, Surf. Sci. **24**, 332 (1971).

²P. W. Palmberg, in *The Structure and Chemistry of Solid Surfaces*, edited by G. A. Somorjai (Wiley, New York, 1969), p. 29.

³J. W. May, Surf. Sci. **17**, 267 (1969).

⁴Ch. Beyreuther and G. Wiech, in *Extended Abstracts of the Fourth International Conference on VUV-Radiation Physics*, edited by E. E. Koch, R. Haensel,

and C. Kunz (Pergamon, Vieweg, 1974), p. 517.

⁵J. Kieser, Z. Phys. B **26**, 1 (1977).

⁶B. Feuerbacher and B. Fitton, Phys. Rev. Lett. **26**, 840 (1971).

⁷R. F. Willis, B. Feuerbacher, and B. Fitton, Phys. Rev. B **4**, 2441 (1971).

⁸A. Bianconi, S. B. M. Hagström, and R. Z. Bachrach, Phys. Rev. B **16**, 5543 (1978).

- ⁹P. M. Williams, D. Latham, and J. Wood, *J. Electron Spectrosc. Relat. Phenom.* **7**, 281 (1975).
- ¹⁰F. R. McFeely, S. P. Kowalczyk, L. Ley, R. G. Cavell, R. A. Pollak, and D. A. Shirley, *Phys. Rev. B* **9**, 5268 (1974).
- ¹¹Y. Baer, *J. Electron Spectrosc. Relat. Phenom.* **24**, 95 (1981).
- ¹²R. F. Willis, B. Fitton, and G. S. Painter, *Phys. Rev. B* **9**, 1926 (1974).
- ¹³G. S. Painter and P. E. Ellis, *Phys. Rev. B* **1**, 4747 (1970).
- ¹⁴J. E. Houston and R. L. Park, *Solid State Commun.* **10**, 91 (1972).
- ¹⁵A. M. Bradshaw and D. Menzel, *Phys. Status Solidi B* **56**, 135 (1973).
- ¹⁶J. Verhoeven and J. Kistemaker, *Surf. Sci.* **50**, 388 (1975).
- ¹⁷C. Webb and P. M. Williams, *Surf. Sci.* **53**, 110 (1975).
- ¹⁸C. Webb, *Vacuum* **27**, 537 (1976).
- ¹⁹J. E. Houston, *Solid State Commun.* **17**, 1165 (1975).
- ²⁰J. Kieser, in *Band Structure Spectroscopy of Metals and Alloys*, edited by P. J. Fabian and L. M. Watson (Academic, New York, 1973), p. 557.
- ²¹R. L. Park and J. E. Houston, *Phys. Rev. B* **6**, 1073 (1972).
- ²²J. E. Houston and R. L. Park, *J. Vac. Sci. Technol.* **9**, 579 (1971).
- ²³K. Wandelt and G. Ertl, *Surf. Sci.* **55**, 403 (1976).
- ²⁴V. Dose and A. Haertl, *Phys. Rev. Lett.* **47**, 132 (1981).
- ²⁵C. Nyberg, *Surf. Sci.* **82**, 165 (1979).
- ²⁶H. Scheidt, M. Glöbl, and V. Dose, *Surf. Sci.* **112**, 97 (1981).
- ²⁷G. Ertl and K. Wandelt, *Z. Naturforsch. Teil A* **29**, 768 (1974).
- ²⁸V. Dose and H. Scheidt, *Appl. Phys.* **19**, 19 (1979).
- ²⁹V. Dose, Th. Fauster, and H. J. Gossmann, *J. Comp. Phys.* **41**, 34 (1981).
- ³⁰V. Dose and H. Scheidt, *Phys. Status Solidi B* **103**, 247 (1981).
- ³¹V. Dose, Th. Fauster, and H. Scheidt, *J. Phys. F* **11**, 1801 (1981).
- ³²C. Boiziau, V. Dose, and H. Scheidt, *Phys. Status Solidi B* **93**, 197 (1979).
- ³³V. Dose, *Appl. Phys.* **14**, 117 (1977).
- ³⁴J. B. Pendry, *Phys. Rev. Lett.* **45**, 1356 (1980).
- ³⁵H. Merz and K. Ulmer, *Z. Phys.* **210**, 92 (1968).
- ³⁶J. K. Lang and Y. Baer, *Rev. Sci. Instrum.* **50**, 221 (1979).
- ³⁷R. R. Turtle and R. J. Liefeld, *Phys. Rev. B* **7**, 344 (1973).
- ³⁸G. Denninger, V. Dose, and H. Scheidt, *Appl. Phys.* **18**, 375 (1979).
- ³⁹V. Dose and G. Reusing, *Appl. Phys.* **23**, 221 (1980).
- ⁴⁰G. Denninger, V. Dose, and H. P. Bonzel, *Phys. Rev. Lett.* **48**, 279 (1982).
- ⁴¹D. Denley, P. Perfetti, R. S. Williams, D. A. Shirley, and J. Stöhr, *Phys. Rev. B* **21**, 2267 (1980).